A triple-GEM detector with pad readout for the inner region of the first LHCb muon station

G. Bencivenni, G. Felici, F. Murtas, P. Valente
Laboratori Nazionali di Frascati - INFN, Frascati, Italy
W. Bonivento[1]**, A. Cardini, A. Lai, D. Pinci**[2]**, B. Saitta**[1,2]
Sezione INFN di Cagliari, Cagliari, Italy
[1]Now at European Laboratory for Particle Physics (CERN), CH1211 Genève 23, Switzerland
[2]and Università degli Studi di Cagliari, Cagliari, Italy
C. Bosio
Sezione INFN di Roma, Roma, Italy

Abstract

We consider a triple-GEM detector with pad readout as candidate for equipping region 1 and 2 of the first muon station (M1) of the LHCb experiment.
This work concentrated on the study of time performance of such a detector. The results are in agreement with a previous measurement of a double-GEM detector when using the standard gas mixture Ar/CO_2 (70/30). In this case the time resolution is such that no high efficiency triggering at LHCb would be possible.
With a new gas mixture, Ar/CO_2/CF_4 (60/20/20), the time performance was found to be considerably improved. With one triple-GEM detector an efficiency of about 96 % (93 %) in a 25 ns (20 ns) time window for minimum ionising particles was obtained. This is adequate for charged particle triggering in the LHCb muon system.

1 Detector requirements

The LHCb muon detector system consists of 5 stations of chambers. The first station (M1) is located in front of the electromagnetic calorimeter while the other four (M2 to M5) are located behind the calorimeters and are separated one from the other by iron walls [1].
The main purpose of the muon system is to give the Level 0 trigger for muons coming from b-flavoured hadron decays. To do this, the trigger requires for a muon candidate to fire all five stations with unambiguous bunch-crossing identification with an efficiency of 95% for the muons inside the acceptance.
Most of the muon system will be equipped with Multi-Wire Proportional-Chambers (MWPC), while the outer part of stations 4 and 5 will be equipped with Resistive Plate Chambers (RPC).
No technology has been chosen yet for the inner part of station 1, where particle rates above 100 kHz/cm^2 are expected. The surface covered by these chambers is 2.9 m^2 per layer.
A detector located in region 1 and 2 should satisfy very tough requirements, in terms of rate capability, efficiency, dead time, number of adjacent pads fired per track and radiation hardness.
To achieve 95% overall trigger efficiency on muons in a bunch crossing interval, each station must have an efficiency of more that 99%. For redundancy, two independent detector layers per station are foreseen, which will be logically OR-ed; therefore, the requirement for the single chamber is of at least 95% efficiency.
The pad cluster size, i.e. the number of adjacent detector pads fired when a track crosses the detector perpendicular to it, should not be larger than 1.2 for a 10x25 mm^2 pad size.
The detector should correctly operate up to a rate of 460 kHz/cm^2 and dead time should be less than 50 ns; this puts stringent limits on both pulse width and on the maximum tolerable discharge rate.
The detector should also operate in a harsh radiation environment. If it is operated with the Ar/CO_2 (70/30) gas mixture and a total gain of 10^4, it would integrate a charge of about 6 C/cm^2.

2 The triple-GEM detector as candidate for regions 1 and 2 of station 1

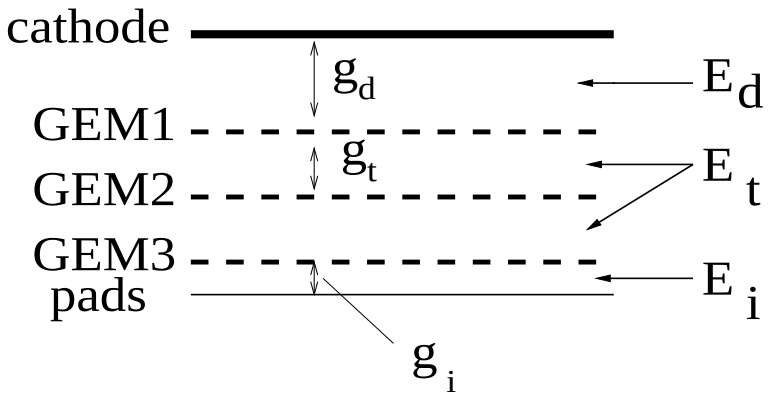

Figure 1: Cross-section of the triple-GEM detector. E_d, E_t and E_i are the drift, transfer and induction fields, respectively; g_d, g_d, and g_i are the drift, transfer and induction gaps, respectively.

Detectors with one or more GEM foil [2] have been extensively studied in the last four years and are currently used as tracking device [3] or as a part of a tracking device [4] in high rate experiments. In particular, when space resolution in the range 100 μm-1 mm is required, they represent a cheaper solution compared to the well established solid state detector technique, being also quite robust against radiation damage.
A GEM is made by a thin (50 μm) kapton foil, copper clad on each side, perforated with high surface density of holes, each one acting as an electron multiplication channel. Each hole has a bi-conical structure with external (internal) diameter of 70 μm (50 μm) and a pitch of 140 μm. The bi-conical shape of

the hole minimises the effect of charging-up of the kapton inside the holes and is a consequence of the double mask process used in standard photolitographic technologies.
A typical voltage difference of 350 to 500 V is applied between the two copper sides, giving fields as high as 100 kV/cm into the holes, resulting in an electron multiplication ranging from 10 to 1000.
Multiple structures realized by assembling two or more GEMs at close distance allow high gains to be reached while minimising the discharge probability.
The triple-GEM detector, which consists of three gas electron multiplier (GEM) foils sandwiched between two conductive planes, one of which, the anode, is segmented in pads and connected to the readout electronics, can be effectively used as tracking detector, with good time and position resolution performances.
A cross-section of this detector is shown in Figure 1.
The ionisation electrons, produced in the gap between the cathode and the first GEM foil (drift gap) by the charged particles crossing the GEM perpendicularly to it, are attracted by electric fields through the three GEM foils where they get multiplied. Once they cross the last GEM foil they drift up to the anode in the so called induction gap, giving rise to an induced current signal on the pads.
Some of the requirements mentioned section 1 were already met by past measurements on double or triple-GEM detectors. Correct detector response of a triple-GEM detector operated at high charged particle flux as expected in LHCb and transverse avalanche size smaller than a mm were measured by the authors of [5].
Discharge probabilities for triple-GEM detectors were measured both with α sources [6] and charged particle beams [3]. However, the discharge probability strongly depends on detector parameters and gas mixture and measurements will have to be performed with the final chosen configuration.
Ageing measurements were so far performed only on double-GEM devices with the Ar/CO_2 (70/30) gas mixture [7]; no degradation of the response was observed up to 70 mC/cm^2.
Only one paper [5] has so far presented a measurement of a double-GEM detector time resolution, with the gas mixture Ar/CO_2 (70/30). The authors of that paper quote a resolution of about 10 ns r.m.s. without software corrections, i.e. such that no high efficiency triggering at LHCb can be performed.
In this note we present a detailed study of detector optimisation for good time performance, both with simulation and beam test measurements, through a detailed investigation of the role played by detector geometry, electric fields and gas mixture.

3 Detector optimisation for LHCb operation

3.1 Time performance

Signal formation in GEM detectors takes place in the induction gap, which behaves in this respect as an ionisation chamber.
Assuming no cross-talk to adjacent pads, the signal induced on a pad by one electron drifting in the induction gap for a time $t_{drift} = g_i/v_{drift}$, where v_{drift} is the drift velocity of electrons and g_i is the induction gap size, is a current pulse of intensity $I = e/t_{drift}$ and duration t_{drift}.
The total signal induced on a pad by a track crossing the GEM is given by the sum of signals due to the single ionisation electrons, amplified by the multiplication through the GEM foils, each one delayed in time by the corresponding electron drift time in the drift gap. The total signal has then to be convoluted with the amplifier response to get the signal at the discriminator input. The discriminator crossing on the signal rising edge gives the time of the event.
The signal rising edge at the amplifier input has a stepwise profile, each step corresponding to the signal of an ionisation cluster (the time spread of electrons within a ionisation cluster is much smaller than the time difference between clusters). Then, the detector time resolution will be determined by the time distribution of the first ionisation clusters and the corresponding signal amplitude fluctuations, both in the ionisation process and in the multiplication through the GEMs. These issues will be addressed in this

section.
For the measurements discussed in this note, very fast (peaking time less than 10 ns) and low noise (equivalent noise charge less than 1500 e^-) amplifiers, already developed for wire chamber operation, were used. Therefore no optimisation of the signal processing chain was performed.

3.1.1 Time distribution of ionisation electrons in the drift gap

The number of ionisation clusters produced in the drift gap follows a Poisson distribution. Therefore, the distance x of the ionisation cluster nearest to the first GEM has the probability distribution $P(x) = n \cdot exp(-nx)$, with $\sigma(x) = 1/n$, where n is the number of ionisation clusters per unit length [2]. In the ideal situation where the first ionisation cluster is always triggered and without the time-walk effect, the detector time resolution would be $\sigma(t) = (n \cdot v_{drift})^{-1}$. The other ionisation clusters have a probability distribution with larger $\sigma(x)$ than the first one, though still proportional to $1/n$.
Thus, in order to optimise the time performance of the detector, a large average atomic number and high drift velocity gas mixture should be used [8].
Two gas mixtures were used in the measurements reported in this note: Ar/CO_2 (70/30), which we used as a reference since it was studied in the past, and $Ar/CO_2/CF_4$ (60/20/20), which we consider to have better time characteristics for the GEM detector. Among the fast and high average atomic number gases, tetrafluoromethane (CF_4) is the most frequently used because it is non-flammable, non-corrosive, non-toxic, and shows a good compatibility with most of metals, plastics and resins used in gaseous detectors construction.
It is important to have a mixture with a high drift velocity at low field, since electron collection by GEM holes is better at low field, as it will be shown in the next section.
The drift velocity for the two mixtures [9, 10] is shown in Figure 2. The $Ar/CO_2/CF_4$ (60/20/20) mixture has 25% higher drift velocity at 3 kV/cm than the Ar/CO_2 (70/30) one. The number of ionisation clusters per cm for the two mixtures is predicted to be 45.5 and 34.3, respectively [11]. Thus, one expects the r.m.s. of the time distribution to improve with the ternary mixture by about 50%.

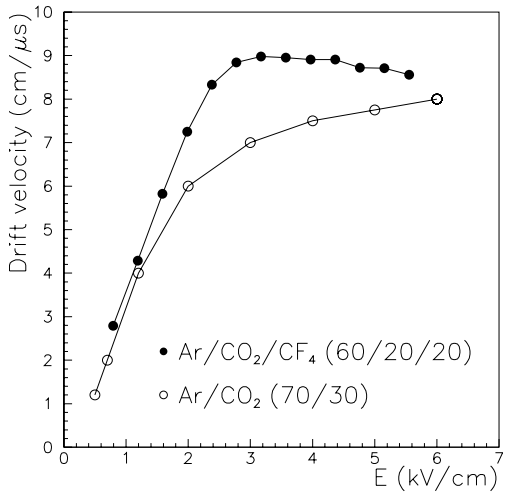

Figure 2: Electron drift velocity for Ar/CO_2 (70/30) and $Ar/CO_2/CF_4$ (60/20/20).

3.1.2 Transmission and multiplication through the first GEM

As explained before, to optimise the time resolution, it is important to maximise the detection efficiency of the first ionisation clusters. The distribution of the number of electrons per ionisation cluster [11] is such that in about 70% of the cases only one electron is produced. This shows that high efficiency in single electron detection is required.

The transmission characteristics of a GEM depend on the drift (E_d) field, the transfer field (E_t), i.e. the field below the GEM, and the voltage applied across it (U_{gem}). To study the dependence of electron transmission on these fields, a detector simulation was developed using a finite element method program to calculate the electric fields [12]. A GEM foil was sandwiched between anode and cathode planes, both at 150 μm distance from the GEM. The drift and transfer field were set to 3 kV/cm while U_{gem} was set to 450 V. Then, electrons were generated at the cathode and tracked through the GEM [13] in the Ar/CO_2 (70/30) gas mixture. No multiplication in the gas was given to the electrons.

For a better understanding of the results two efficiencies were defined. The fraction of electrons still present in the GEM holes at the median GEM plane, i.e. the plane parallel to the GEM foil at half distance between the top and bottom GEM copper layers, was defined as the *collection* efficiency and the fraction of electrons which were present in the GEM holes at the median GEM plane and were arriving up to the anode was defined as the *extraction* efficiency. The product of the two is the *total* efficiency.

Figure 3(a) shows that the collection and the total efficiencies decrease at high drift field values and

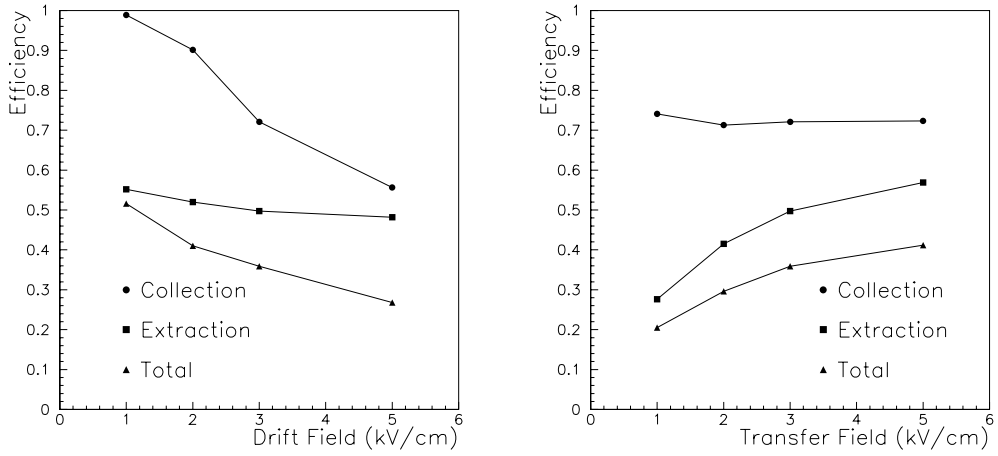

(a) (b)

Figure 3: Simulated collection, extraction and total efficiency through a GEM foil, as a function of drift field (a) and of transfer field (b).

this can be understood as a defocusing of field lines above the GEM bringing the ionisation electrons to directly impinge on the upper copper layer. Figure 3(b) shows that the extraction and total efficiency increase at high transfer fields. This is understood in terms of a better electron extraction capability from the lower side of the GEM (Figure 3(b)).

The two figures also show that the top and bottom side properties of the GEM are marginally influenced by the bottom and top fields, respectively.

They also show that no matter what the amplification in the gas is, the efficiency for single electron detection at fields of 3 kV/cm, which are typical for triple-GEM operation, cannot be larger then 70 %.

The collection and total efficiencies show a small increase with U_{gem} (Figure 4). This is understood in terms of a better electron collection inside the GEM holes. No deterioration of the extraction efficiency

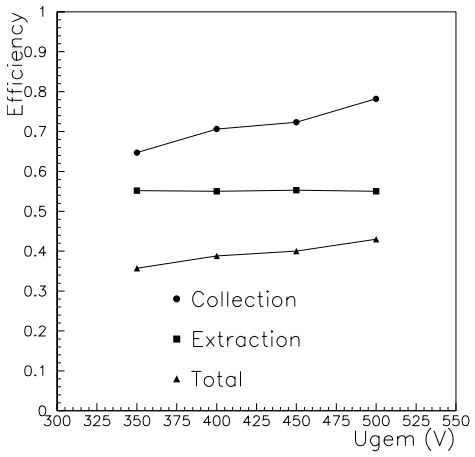

Figure 4: Simulated collection, extraction and total efficiency for an electron produced 150 μm a GEM foil, as a function of the GEM voltage, without amplification in the gas.

is observed with increasing U_{gem}.
To improve the detection efficiency of the first clusters and reduce the influence of the time-walk effect it is useful to have a high total GEM gain.
To achieve a given total gain, instead of raising the three GEM voltages at the same time, it is better to increase only U_{gem1}. Beyond improving slightly collection efficiency, this minimises gain fluctuations where they are larger, i.e. in the first gap where a small charge is produced. In this way the influence of the *bi-gem* effect, i.e. the amplification of the ionisation electrons produced in the first transfer gap, out of time with respect to those coming from the drift gap by $\Delta t = g_t/v_{drift}$, where g_t is the transfer gap size, is also reduced.
This choice might also be safer from the point of view of discharge probability since previous studies [6] indicate that discharge probability depends both on total gain and on voltage of the last GEM.

3.2 Pad cluster size

To keep the pad cluster size small, two effects should be considered: cross-talk to adjacent pads by direct induction, which is minimised keeping the induction gap small, and capacitive cross-talk, which is minimised when the pad cross capacitance is small, i.e. with a small induction gap, and when the amplifier input impedance is small.

3.3 Selection of detector parameters

It is clear from the previous discussion that detector optimisation for LHCb operation is the result of a compromise among some conflicting requirements.
The size of the drift gap g_d has to be large enough to minimise inefficiencies in charged particle detection but should be kept small to reduce the dead time due to pulse width. With a 3 mm gap and fast amplifiers, the pulse width would be less than 40-50 nsec, which satisfies the requirements.
Since the longitudinal diffusion is minimal due to the small drift path of the electrons in the detector, the only effect of the transfer gap is to give a delay to the detected pulse. However, to minimise the impact of the above mentioned *bi-gem* effect, the size of the transfer gap g_t was kept to 2 mm.
Given the fast amplifiers we used in this test, the size of the induction gap g_i should be small to increase the amount of charge integrated by the amplifier and to reduce the cross-talk fraction (with a charge integrating amplifier with large integration time constant the gap size would not matter). A lower limit

to the size of the induction gap was considered to be between 1 and 1.5 mm, to minimise the discharge probability, which is likely to be affected by the gap width itself [6].
The best values for the electric fields E_d, E_t and U_{gem} were experimentally determined by optimising the detector efficiency in a given time window. The value of E_i was fixed during these measurements at 5 kV/cm.
The threshold value was kept small to reduce the influence of the time-walk effect and to increase the probability to trigger on the first ionisation cluster.

4 Experimental measurements

4.1 Detector construction

For the test described in this note, two similar detector prototypes, one built by INFN Cagliari and one built by INFN Frascati, which will be labelled A and B in the following, were used.
The three 10×10 cm^2 active surface GEM foils [14] were fixed on G10 frames with an epoxy glue

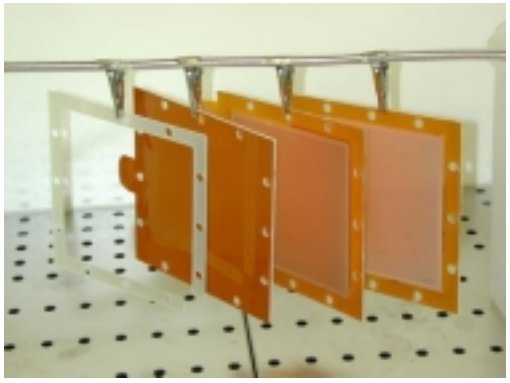

Figure 5: The three GEMs glued on the G10 frames of different thicknesses.

(Figure 5). The anode was segmented in 6×16 mm^2 pads (Figure 6(a)). The cathode was made of a kapton foil, with copper on one side, glued on a similar frame (Figure 6(b)). All frames were then fixed to the G10 box with nylon screws. The G10 box acted also as gas container.
The high voltage was fed with individual channels to the top and bottom side of each GEM and to the cathode through one 10 MΩ (two 1 MΩ) resistors for detector A (B).
The gas flow rate was set to 2.2 l/h.

4.2 Readout electronics

For this test, fast amplifiers already developed for wire chambers were used. For detector A, 12 pads were equipped with a PNPI design [15] amplifier, already used for tests of prototypes of muon chambers for LHCb; for detector B, 15 pads were equipped with the KLOE-VTX chip [16].
For few pF input capacitance, such as for the pads of our triple-GEM detector, the characteristics of these amplifiers, were quite similar: 5 ns peaking time, 1300 e^- r.m.s. equivalent noise charge, 10 mV/fC sensitivity and 25 Ω (110 Ω) input impedance for detector A (B) for a delta pulse input.

4.3 Beam test setup

The measurements were performed at the PS T11 hadron beam facility at CERN. The beam was composed of 2 to 4 GeV pions and the rate was set at about 1 kHz/cm^2.
The trigger consisted of the coincidence of three scintillators $S1 \otimes S2 \otimes S3$, 10×10 cm^2, 15×15 cm^2 and 1×3 cm^2 respectively, centred on the beam axis, about 1 m apart one from the other. The coincidence

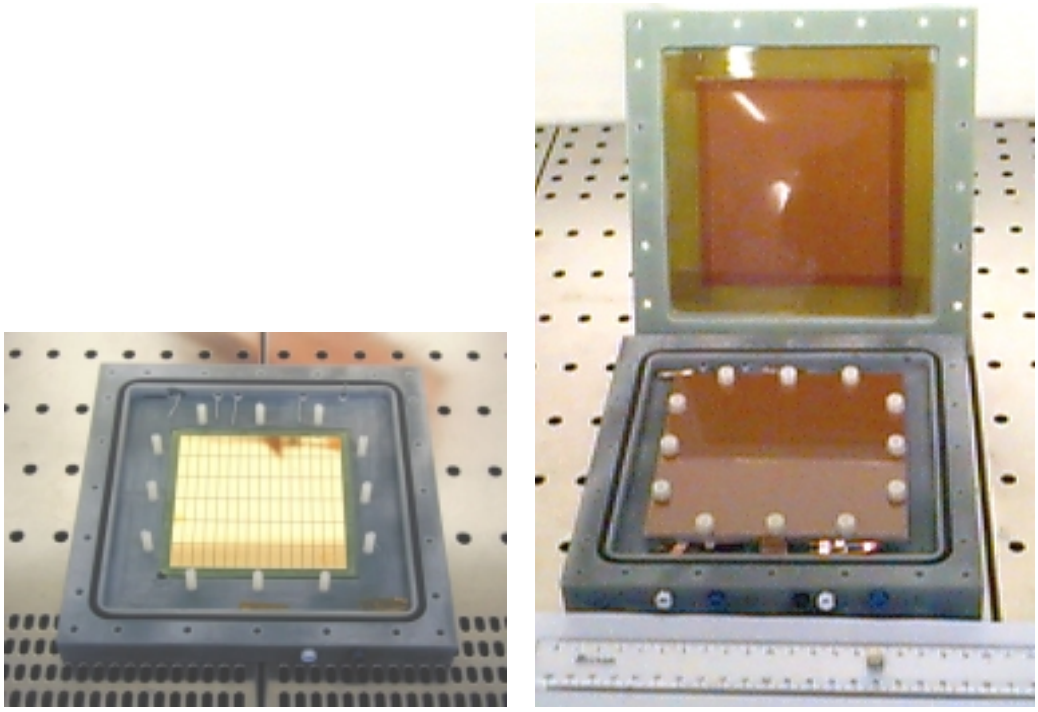

(a) (b)

Figure 6: (a) Readout pads mounted on the G10 box and (b) the three GEMs stacked in the box. The box acts as both GEM support and gas container.

of the S1 and S2 signals was sent to a constant fraction discriminator and delayed to give the common stop to a 16-bit multi-hit TDC, with 1 ns resolution and 20 ns double edge resolution.
The discriminator threshold on the triple-GEM detector signal was set to about 15 mV, in order to have the noise counts below 100Hz.
All signals were sent to a 12 bits charge ADC with 50 fC/count sensitivity.
Detector A (B) was placed 5 cm before (after) S2. The beam was focused near S1 and monitored through a scintillator hodoscope, placed in between S1 and S2, with horizontal and vertical tiles of 1 cm width.
For each run 20,000 triggers were collected.

4.4 Results

For the data analysis, events with large ADC signals in the trigger scintillators, which might have originated from two tracks coming within the ADC gate of 200 ns were rejected.
For efficiency measurement, the time of the event was defined as the first time of threshold crossing among those channels which were above threshold.
The two chambers showed very similar performances in terms of efficiency and pad cluster size. Therefore, in the following no mention to the chamber type will be given anymore.
In our detectors no trips occurred during the test beam period, using a current limit of 2 μA and a trip time of 0.1 s on the high voltage power supply and no current was observed with the HV power supply sensitivity of 100 nA. However, a detailed study of discharge rate was not performed and will be the subject of a future publication.

4.4.1 Efficiency

Figure 7(a) and Figure 7(b) show the time distributions obtained with the Ar/CO_2 and Ar/CO_2/CF_4 gas mixtures, respectively, for U_{gem2} =$U_{gem3} = 390$ V, $U_{gem1} = 460$ V, $E_d = 3$ kV/cm and $E_t = 3$ kV/cm ($E_t = 4$ kV/cm for figure 7(b)).
The two figures show a clear asymmetry with one tail on the left hand side and one of different size on the left hand side. The time scale in the plot refers to the TDC common stop, so the entries at the right of the peak correspond to events early in time.
The tail on the left of the peak is mainly due to small amplitude signals, as shown in Figure 8 for one run

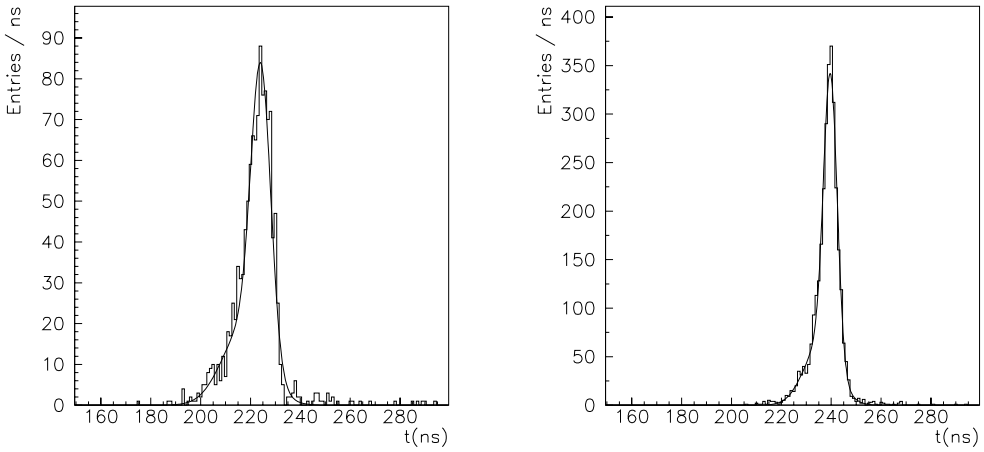

(a) (b)

Figure 7: Time distributions with Ar/CO_2 (70/30) (a) and Ar/CO_2/CF_4 (60/20/20) (b). The r.m.s. of the two distributions are 9.7 and 5.9 ns, respectively. A fit with a sum of two Gaussian functions is superimposed to the plots.

with Ar/CO_2/CF_4, with $E_d = 3$ kV/cm, U_{gem2} =$U_{gem3} = 390$ V, $E_t = 4$ kV/cm and $U_{gem1} = 450$ V. This can be interpreted as being tracks producing a small number of ionisation clusters in the drift gap and partly as time-walk effect.
The entries on the right of the peak are explained by the *bi-GEM effect*, mentioned in section 3.1.2. They amount to 1 to 2% of the total number of entries, rather independent of the U_{gem1} value. The choice of the first triggered pad in the event somewhat amplifies the presence of these early signals. Indeed, when events with only one triggered pad are selected, so that there is no ambiguity in the choice of the pad giving the trigger time, the fraction of the early hits is reduced by 40% while the r.m.s. of the time distribution is only 3.5% smaller. This also shows that the first triggered pad is a good estimator for the time of the event.
The r.m.s. of the distribution in Figure 7(a) is 9.7 ns. For comparison, a measurement by other authors [5] obtained with a bi-GEM detector and a four times slower rise-time amplifier gave a σ of one Gaussian fit of 9.9 ns without software corrections. A fit with the sum of two Gaussian functions was superimposed to the distribution of Figure 7(a), giving a σ of 3.9 ns for the narrower of the two Gaussian functions.
The r.m.s. of the distribution in Figure 7(b) is 5.9 ns. The two-Gaussian fit gave a σ of 2.8 ns for the narrower of the two Gaussian functions.
The different mean value of the time distributions with the two gas mixtures is consistent with the difference in the drift velocity, taking also into account the drift of electrons in the two transfer gaps.
This observed improvement on the r.m.s. with the ternary mixture of about 40% is in rough agreement

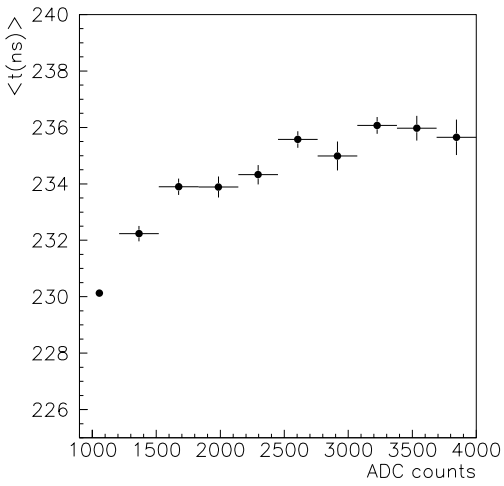

Figure 8: Time vs. signal amplitude, as measured by the charge ADC in a run with the Ar/CO_2/CF_4 gas mixture.

with expectations, as follows from the discussion of section 3.1.1.
Even if the absolute GEM gain was not determined, the GEM gain ratio between the two mixtures could be extracted from the ADC spectra in two runs taken with U_{gem2} =U_{gem3} = 390 V, U_{gem1} = 450 V and the same drift and induction fields. The binary mixture turned out to give 35 % larger gain than the ternary one; once the different drift velocity and primary ionisation are taken into account the effect becomes 48 %. This different GEM gain can explain the smaller improvement in time resolution observed in the data compared to expectations.
The lower gain of the ternary mixture might also imply a smaller discharge probability than with the binary one, at the same GEM voltage configuration.

Effect of the drift field

The plot in Figure 9(a) shows for the Ar/CO_2/CF_4 gas mixture detector efficiencies measured in a 300 ns (which we call global efficiency) and 25 ns time window as a function of the drift field E_d, when E_{t1} =E_{t2} = 4 kV/cm and U_{gem1} =U_{gem2} =U_{gem3} = 375 V. For E_d = 3 kV/cm a global efficiency of a 96% is reached, decreasing to 87% for 25 ns. The plot displays an optimum value, at about 3 kV/cm. At low field values the efficiency loss can be explained by the low drift velocity and at high fields by the defocusing effect of field lines, as seen also in the simulation (see section 3.1.2).
A similar behaviour was observed for the other gas mixture.

Effect of the transfer field

The efficiencies are shown in Figure 9(b) as a function of the transfer field value, with E_d = 3 kV/cm and $U_{gem1} = U_{gem2} = U_{gem3} = 375$ V.
The plot shows an optimum value at about 3 kV/cm, where the efficiencies are 97 % and 87 % for the 300 ns and the 25 ns time window, respectively.
At small transfer field we observed an efficiency loss, which is well described by the simulation (see section 3.1.2). At high transfer field the efficiency drops. This can be explained by a smaller collection efficiency from the second GEM and third GEM.
A similar behaviour is observed for the other gas mixture.

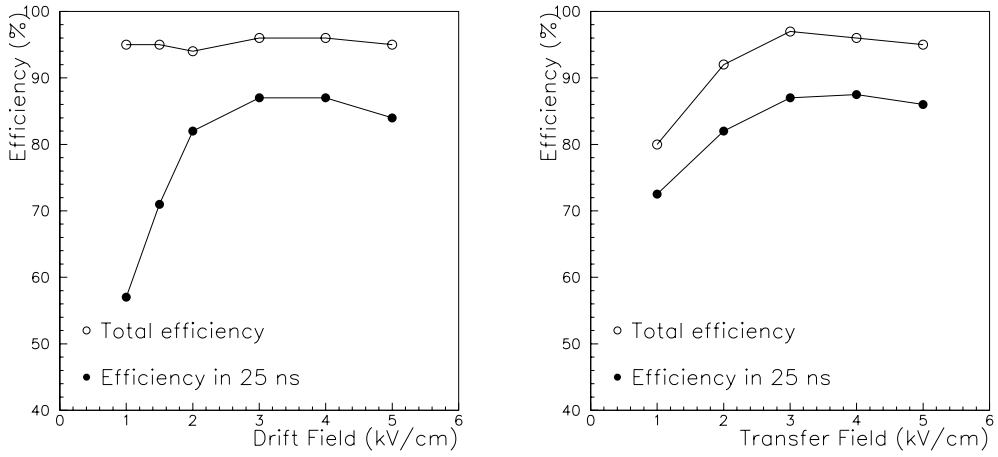

(a) (b)

Figure 9: Detection efficiency as a function of (a) the drift field and of (b) the transfer field, with $E_{t1} = E_{t2}$, for the $Ar/CO_2/CF_4$ mixture.

Effect of GEM1 voltage

The efficiencies for the various time windows as function of U_{gem1} are shown in Figure 10(a) (b)) for the Ar/CO_2 ($Ar/CO_2/CF_4$) gas mixture, for $E_d = 3$ kV/cm, $U_{gem2} = U_{gem3} = 390$ V, $E_t = 4$ kV/cm. Efficiencies of 90 % (85 %) in 25 ns (20 ns) window were obtained at the highest value of U_{gem1} with Ar/CO_2 while of 96% (93%) in a 25 ns (20 ns) window with $Ar/CO_2/CF_4$, confirming the better timing properties of the CF_4 based gas mixture.

The choice of increasing the gain of the first GEM rather than of all three GEMs altogether to improve

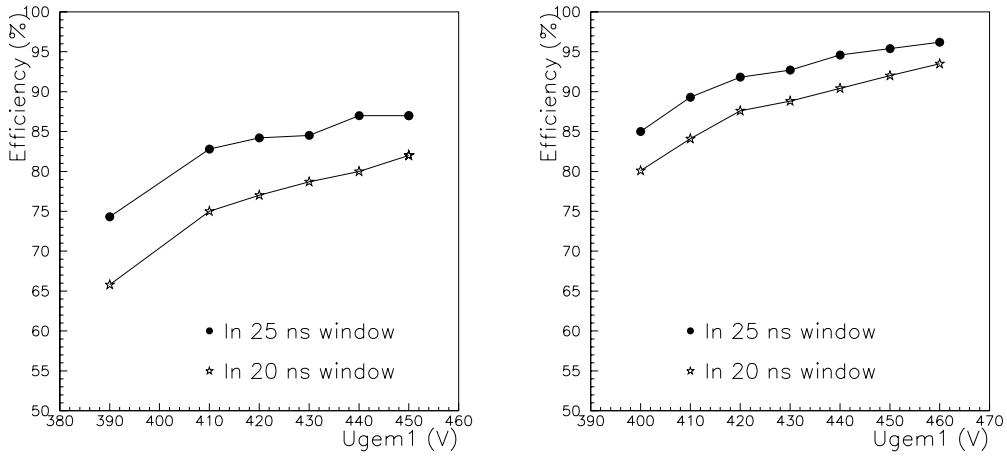

(a) (b)

Figure 10: Detector efficiencies as a function of U_{gem1} with Ar/CO_2 (a) and $Ar/CO_2/CF_4$ (b).

the time performance, as discussed in section 3.1.2, finds also some justification from the data. Indeed, since the gain of a GEM stage is an exponential function of the voltage, the total gain depends on the sum of the three GEM voltages. Two runs, with the Ar/CO_2 mixture, were taken with different voltage configurations of the three GEMs but the same total gain: run i) with $U_{gem1} = 410$ V, $U_{gem2} = 390$ V and $U_{gem3} = 390$ V and run ii) with $U_{gem1} = 390$ V, $U_{gem2} = 400$ V and $U_{gem3} = 400$ V. The two measured gains from ADC spectra are, as expected, equal within few %. Run i) has a 50% smaller *bi-gem* event fraction, the σ of the main peak of the time distribution is 10 % narrower and the r.m.s. of the distribution 11 % narrower.
In summary, the efficiency plots as function of various parameters display a smooth behaviour. This is a good indication for stability in long time operation of the detector.

4.4.2 Pad cluster size

The pad dimension used in this test was $6 \times 16\ mm^2$, i.e. smaller than that needed for the LHCb detector. The obtained pad cluster size at U_{gem1}=460 V is, for the Ar/CO_2 ($Ar/CO_2/CF_4$) gas mixture, 1.6 (1.5). Since the discriminator threshold was kept fixed during the whole beam test, the pad cluster size increased with signal amplitude. For example, it increased by 17% when U_{gem1} went from 400 V to 460 V.
As a rough estimate of cluster size with larger pads, it was possible in the offline analysis to add three pads together, obtaining a *software pad* of size 18×16 mm^2. The pad cluster size so obtained was 1.1 for both mixtures.

5 Future developments

The results of this test are quite encouraging.
However, to establish whether the triple-GEM detector fulfils or not all LHCb requirements for region 1 and 2 of station 1 some other studies are planned for the near future:

- Study of detector performance at the rate expected at high luminosity (about 1 MHz/cm^2), to be performed at PSI;
- Local ageing test of the detector, to be performed using a high intensity (up to 1 MHz/mm^2) and low energy (6.4 KeV) X-ray tube at LNF;
- Global ageing test irradiating a larger area;
- Direct measurement of the spark rate with the optimal configuration of electric fields;
- Test of the electronics foreseen for the LHCb wire chambers;
- Test the effect of OR-ing two chambers;
- Tuning of the gas mixture, detector geometry and electric fields to improve further the time resolution

6 Conclusions

Triple-GEM detectors equipped with pad readout, with an $Ar/CO_2/CF_4$ (60/20/20) gas mixture, showed good time performance, resulting in a time distribution r.m.s. of 6 ns and an efficiency of 96 % (93 %) in a 25 ns (20 ns) time window. These performances allow this type of detector to be considered as candidate for region 1 and 2 of the of the first station of the LHCb muon detector.
Studies aiming at investigating the stability of these detectors under high charged-particle rate and their aging properties are in progress.

7 Acknowledgements

The authors would like to thank F. Sauli for useful discussions. This work would not have been possible without the support of the technical staff both at INFN Cagliari and at LNF, and in particular of: M. Arba and M. Tuveri (INFN Cagliari) for the realization of the mechanics of the Cagliari prototype; D. Marras (INFN Cagliari) for the design and the assembly of the front-end electronics of the Cagliari prototype; B. Ortenzi (LNF) for the design of the detector box of the Frascati prototypes; E. Iacuessa and S. Valeri for the realization of the mechanics of the Frascati prototypes; the LNF Electronics Pool for the realization of the front-end electronics of the Frascati prototypes.

References

[1] LHCb Muon System Technical Design Report, CERN LHCC 2001-010, LHCb TDR 4, (2001).

[2] F. Sauli, Nucl. Instrum. Meth. **A386**, 531 (1997).

[3] S. Bachmann et al., CERN-EP/2000-116, 31 August 2000.

[4] T.Zeuner,Nucl. Instrum. Meth. **A446**, 324 (2000)

[5] A. Bressan et al., Nucl. Instrum. Meth. **A425**, 262 (1999).

[6] S. Bachmann et al., CERN-EP/2000-151, 11 December 2000.

[7] H.R.Schmidt et al, ALICE note 1999-56.

[8] F.Sauli, CERN Report 77-09 (1977).

[9] S. Bachmann et al., Nucl. Instrum. Meth. **A438**, 376 (1999).

[10] U. Becker et al., "Gas R&D Home Page (http://cyclotron.mit.edu/drift)".

[11] I.Smirnov, HEED, program to compute energy loss of fast particles in gas, Version 1.01, CERN.

[12] MAXWELL 3d extractor, ANSOFT.

[13] R.Veenhof, GARFIELD, a drift chamber simulation program, Version 7.02, CERN.

[14] A. Gandi, Laboratory of Photomechanical Techniques and Printed Circuits, EST-SM-CI Section, CERN, Geneva, Switzerland.

[15] A.Vorobyov et al, LHCb note 2000-003.

[16] R.J. Yarema et al.,IEEE Trans. Nucl. Sci.,**39**, No. 4, 742(1992)